Flexural and shear behaviour of profiled double skin composite elements

K. M. Anwar Hossain†

Department of Civil Engineering, Ryerson University, Toronto, Canada

H. D. Wright†

Department of Civil Engineering, University of Strathclyde, Glasgow, UK

Abstract.   Double skin composite element (DSCE) is a novel form of construction comprising two skins of profiled steel sheeting with an infill of concrete. DSCEs are thought to be applicable as shear or core walls in a building where they can resist in-plane loads. In this paper, the behaviour of DSCE subjected to combined bending and shear deformation is described. Small-scale model tests on DSCEs manufactured from micro-concrete and very thin sheeting were conducted to investigate the flexural and shear behaviour along with analytical analysis. The model tests provided information on the strength, stiffness, strain conditions and failure modes of DSCEs. Detailed development of analytical models for strength and stiffness and their performance validation by model tests are presented.

Key words: double skin composite element, bending and shear strength, profiled steel sheeting, sheet-concrete interaction, analytical models

1. Introduction

The concept of double skin composite element (DSCE) originated from the use of composite flooring with profiled steel deck in buildings (Wright *et al.* 1992). Fig. 1 shows a schematic diagram of the novel construction system, which comprises two skins of profiled steel sheeting and an infill of concrete. The advantages of this system arise from the type of construction where profiled steel sheeting acts as a formwork for in-fill concrete (Gallocher 1993). In the service stage, profiled steel sheeting also acts as reinforcement. DSCEs have many advantages when used in conjunction with composite flooring and are thought to be especially applicable as shear or core walls in steel framed buildings (Fig. 1). They have potential in concrete buildings, basements and blast resist structures.

Other forms of DSCE have been proposed earlier for submerged tube tunnel, offshore and defence structures. The DSC system devised for submerged tube tunnels consisted of a double skin steel plated construction secured by welding headed studs at suitable intervals anchored in a concrete infill (Narayanan *et al.* 1987). The spacing of studs was used to control the local buckling of steel sheets
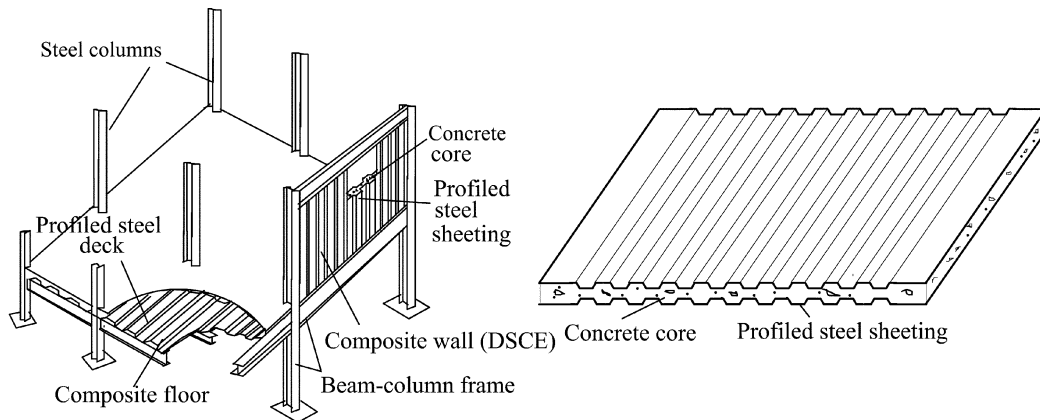
---

†Professor

Fig. 1 Double skin composite element (DSCE) and its application in a building

under loading. In conventional concrete tube tunnels, an outer steel layer is required to ensure water tightness but with external steel skin reinforcements this would not be required. Naraynan *et al.* (1987) concluded that the applications of the system were not limited to submerged tunnels but had wider general applications in construction. Wright *et al.* (1991) reported experimental investigations and described design developments on double skin composite beams and columns. Design recommendations were made to avoid buckling of compression plate, for basic design shear strength and for combined axial and bending effects.

The idea of using composite steel and concrete walls to resist offshore loads was introduced by the Hitachi Shipbuilding and Engineering Company (Adams 1987). Link and Elwi (1995) studied the ultimate and post-peak capacity of composite-steel plate walls subjected to transverse and longitudinal loading. The project investigated simple sandwich walls consists of double skin steel plates with concrete infill. The composite action was provided by the internal steel diaphragm plates connecting the two outer skin plates. The main application of these composite walls lies in the design of offshore structures subjected to large forces from wave action or moving ice.

Yarushalmi (1988) in the United States proposed a form of composite walling known as the ASP Construction System. The development of the system was primarily for use in protective structures from blast resistance and weapons. The proposed wall element consists of exterior steel panels and diagonal interior steel lacing panels with a concrete fill. The walls vary in thickness from 8 to 16 inches and can be filled with concrete, crushed stone or sand. The performance of ASP system was assessed against fragments generated by near miss air bombs. High resistance to penetration was achieved as spalling of the inside surfaces was prevented by the inner steel surface. Further tests investigated the systems dynamic response, protection against chain detonations and the effects of direct rocket hits where 50 percent less penetration occurred than in massive concrete.

Previous research concentrated on the axial load behaviour of profiled DSCEs as composite walls (Wright and Gallocher 1995, Wright 1998, Hossain 2000, Bradford *et al.* 1998). The behaviour was associated with the difficulty in the transfer of load between the steel skins and concrete core, the buckling of the steel sheeting and reduced capacity of the concrete core due to profiling. Taking into account these factors, a design equation for the axial capacity of composite walls subjected to nominally concentric loading was developed (Wright and Gallocher 1995, Wright 1998).

Comprehensive research has been carried out on profiled DSCEs so that they can be used as lateral
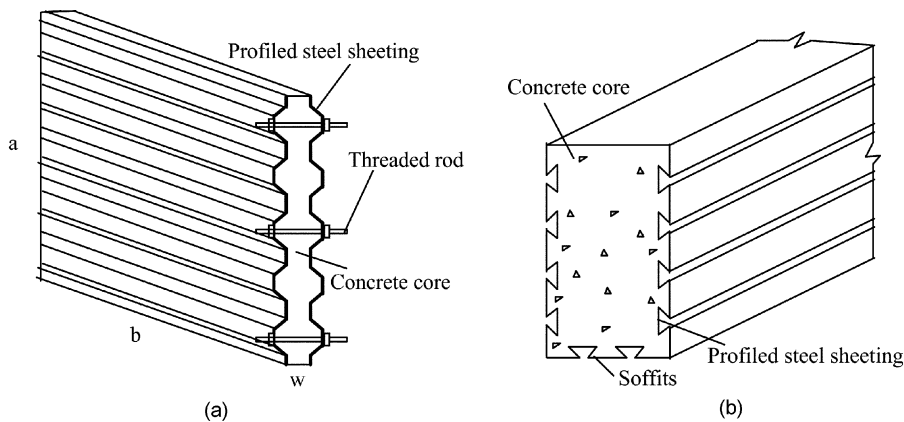
Fig. 2(a) DSCEs under investigation, (b) Profiled composite beam (PCB)

load resisting elements or shear walls in buildings (Hossain and Wright 1995, 1998a, 1998b, 2004a). Depending on structural configuration, the mode of action of such shear walls may be governed by either pure shear or combined shear and bending. In a framed-shear wall building where the boundary frame beams and columns are assumed pinned, the infill composite wall panel resists lateral load by pure shear action. Design guidelines associated with the use of composite walls in a framed shear wall building under monotonic as well as cyclic shear loading conditions have been developed based on experimental, analytical and finite element investigations (Hossain and Wright 2004b, 2004c).

This paper presents the experimental and theoretical investigations on the behaviour of DSCEs subjected to combined bending and shear loading. DSCEs were considered as beams (Fig. 2a) similar to the profiled composite beams (PCB) (Fig. 2b) proposed by Oehlers (1993) and Oehlers *et al.* (1994) where profiled steel decking was used as permanent and integral shuttering for the sides and soffits of the reinforced concrete beam.

Oehlers (1993) suggested that side profiled sheets increased shear strength and shear ductility as well as substantially increasing the flexural strength without loss of ductility. PCBs were more ductile than reinforced concrete beams of similar flexural strengths and the deflections were reduced as much as 40% due to reduced shrinkage and creep in the encased concrete, allowing an increase in span-to-depth ratio of the order of 20%. However, the flexural strength of PCBs was affected by the local buckling of the sheeting between the ribs of the profiled sheeting but the shear bond failure had only a small effect on the ultimate strength.

The side profiled sheets were more effective in PCBs (Fig. 2b) as they were integral parts of the soffits and were also joined together with additional connections (bracing). In the proposed DSCEs (Fig. 2a), sheets are independent and connected only through the threaded rods. As a result, buckling of sheeting and strain characteristics within the DSCEs will be different compared with PCBs. The presence or absence of flexural reinforcing bars in PCBs and DSCEs respectively will also make a difference in the strength and ductility characteristics of the two systems. However, DSCEs are intended to be used as a walling system with lower width to depth ratio compared to PCBs. As a result deep beam action may be prominent in a DSCE shear wall subjected to cantilever bending action.

In this paper, results of extensive experimental investigations on DSCEs are analyzed to understand the general behaviour including bending and shear strength, strain characteristics and modes of failure. The effects of span-to-depth ratio, mode of connections and loading arrangements are also investigated.

The paper also presents the development of analytical models for the flexural and shear strength of DSCEs.

2. Experimental studies

Small-scale models of DSCEs manufactured from micro-concrete and 0.45 mm thick profiled steel sheeting having varying span-to-depth (*b/a*) and depth-to-width (*a/w*) ratios were tested (Fig. 2a and Table 1). Model profiled sheets were manufactured in-house by using a specially fabricated fly press (Fig. 3). The models were divided into three series A, B and C based on mode of connections and loading arrangements. Tests provided information on load-deformation response, strain characteristics including flexural, shear and principal strains, and overall failure characteristics of DSCEs. They also provided information on the effect of *b/a* and *a/w* on the behaviour of DSCE as beams.

Table 1 Dimensions and material properties of the DSCE models

Test series	DSCE beam model	Effective span (*b*) mm	Depth (*a*) mm	Width (*w*) crest	trough mm	*b/a*	*a/w* crest	trough	Bearing plate
A	A1	590	250	30	14	2.36	8.33	17.86	No
	A2	590	140	30	14	4.21	4.66	10.00	No
B	B1	590	240	30	14	2.46	8.00	17.14	Yes
	B1a	590	240	30	14	2.46	8.00	17.14	Yes
	B2	590	200	30	14	2.95	6.67	14.29	Yes
	B2a	590	200	30	14	2.95	6.67	14.29	Yes
	B3	590	140	30	14	4.21	4.66	10.00	Yes
	B3a	590	140	30	14	4.21	4.66	10.00	Yes
	B4	590	100	30	14	5.90	3.33	7.14	Yes
	B4a	590	100	30	14	5.90	3.33	7.14	Yes
C	C1	590	240	30	14	2.46	8.00	17.14	Yes
	C2	590	140	30	14	4.21	4.67	10.00	Yes
	C3	590	100	30	14	5.90	3.33	7.14	Yes

f'_c = 18 MPa (Series A); 21 MPa (Series B and C)
v_c = 0.18; v_s = 0.25; E_c = 18 kN/mm^2; E_s = 185 kN/mm^2; f_y = 375 MPa (Series A, B and C)

Fig. 3 Manufacture of model profiled sheets in a fly press

2.1. Dimensions of DSCE models

Schematic diagrams of typical DSCE models are presented in Figs. 4(a-b). Pairs of profiled steel sheeting were connected together at the ends and at the centre by threaded rods passing through spacers. Test Series A was performed without bearing plates at the point of application of concentrated load and at the supports whereas in Series B and C, bearing plates were used. Bearing plates connected the pair of profiled sheets by threaded rods with nuts and washers arrangements as shown in Figs. 4(a-b) and hence strengthened the support and loading points against localised bearing failure.

Series A and B were tested under single point loading while Series C was tested under two-point loading conditions. Detailed dimensions of the thirteen DSCE models are tabulated in Table 1. The length of all the DSCE models was kept constant at 650 mm providing an effective span (*b*) of 590 mm
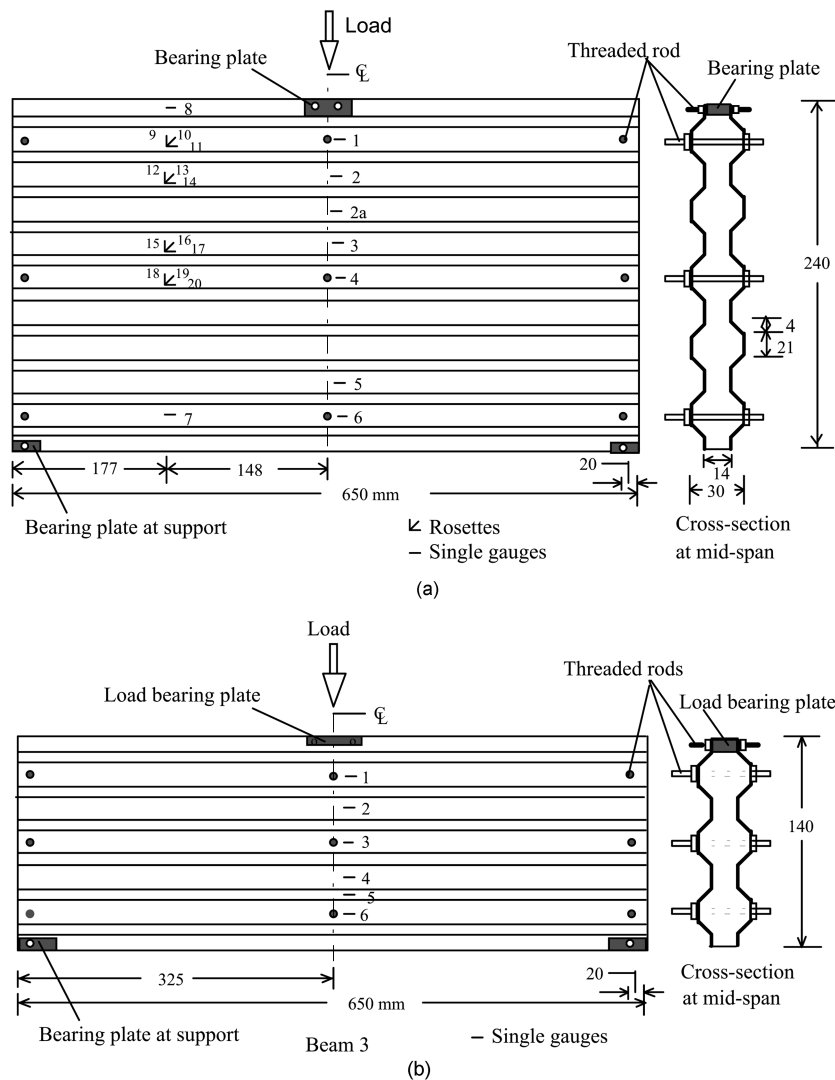

Fig. 4 (a) Details of a DSCE model (B1: Series B), (b) Details of a DSCE model (B3: Series B)
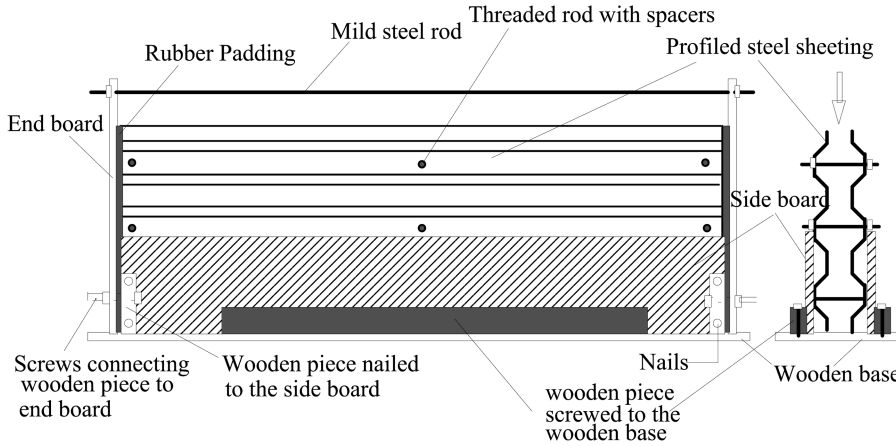
Fig. 5 Casting of DSCE models with micro-concrete

between the supports. *b/a* of the DSCE models was varied from 2.36 to 5.90 to simulate flexural or shear dominated failures, while *a/w* of the trough section ranged between 7.14 and 17.14.

2.2. Casting and curing of DSCE models

The steel sheets were connected together using all the threaded rods at the centre and ends, maintaining correct spacing with the help of spacers. The sheeting assembly was then placed on a wooden mould having a wooden base and side boards as shown in Fig. 5. The micro-concrete was machine mixed and poured into the mould and then compacted on a vibrating table. Control specimens in the form of cubes and cylinders were also cast at the same time to determine the properties of the micro-concrete. The wet density of concrete was also measured as a compaction control for different model specimens. The DSCE models and control specimens were removed from the moulds after 24 hours and then cured in dry air until they were tested.

The steel and concrete properties of the DSCE specimens are presented in Table 1. The yield strength (f_y), modulus of elasticity (E_s) and Poisson's ratio (v_s) of the steel sheeting were determined from coupon tests.

2.3. Instrumentation and experimental set-up

Single and rosette strain gauges were installed at strategic locations on the model specimens. Typical strain gauge locations in B1 and B3 models of test Series B are shown in Figs. 4(a-b). The strain gauges were installed on the steel surface.

A schematic diagram of the experimental set-up under single point loading is shown in Fig. 6. DSCE models were placed between the guide angles, which provided lateral supports to keep the models in a vertically upright position. Padding was used between the specimen and the guide angles. The assembly of guide angles and roller and pin supports were set up on an I-beam base strengthened by stiffening plates. The specimens were then tested by applying a concentrated load at mid span (for Series A and B) or two point loading (for Series C). Dial gauges or LVDTs were used to measure central deflection. The strain and displacements were recorded by a computer controlled data acquisition system.
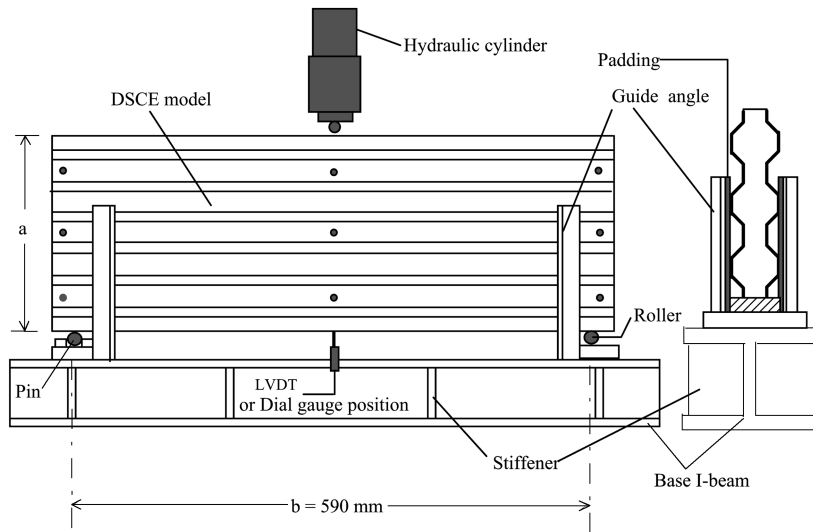
Fig. 6 Schematic diagram of a typical experimental set-up with single point loading

2.4. Test observations

Tests were performed by applying compressive loads in increments and at each load increment, the strains and displacements were recorded. DSCE model A1 suffered local crushing of concrete near the concentrated load application point. Model A1 failed with the subsequent development of cracks at mid span and near the support and crushing of concrete at the loaded point and at the supports. Figs. 7(a-b) show Model A1 before and after failure and Fig. 7(c) shows the crack patterns in the concrete core. The loading roller punched into the DSCE beam at the loaded point due to the absence of a bearing plate. The profiled steel sheeting buckled outward and twisted, directly beneath the loading point. The separation of the sheeting started from the centre and extended towards the ends. Buckling and twisting of the sheeting were restricted to the compression zone directly beneath the loading point.

The local crushing at the loaded point and at the supports was avoided in DSCE models in Series B and C as they incorporated bearing plates. Figs. 7(d-e) show the failure of model B3 and crack patterns in the concrete core. The failure of the DSCE models was governed by either flexure or shear modes depending on the type of connection and dimensions of the beams. Typical variation of central deflections in models B1 and B3 (Series B) is shown in Fig. 8.

2.5. Analysis of strains

2.5.1. Flexural strains at mid span

The variation of flexural strains across the depth of DSCE beam B1 (Series B) at mid span in the pre and post cracking stages is shown in Figs. 9(a-b). The variation was similar to that of an ideal beam with maximum stresses at the top and bottom fibres with zero values at the neutral axis. The flexural strain in the bottom fibre exceeded the limiting concrete tensile strain (0.00015) at about 4.5 kN.

The variation of flexural strains in DSCE beam B3 (Series B) is presented in Fig. 9(c), and shows similar behaviour to B1. The bottom fibre strain exceeded the tensile cracking strain of concrete at about 2 kN. The tensile strain at gauge g-6 (near the bottom fibre) exceeded the yield strain of steel at
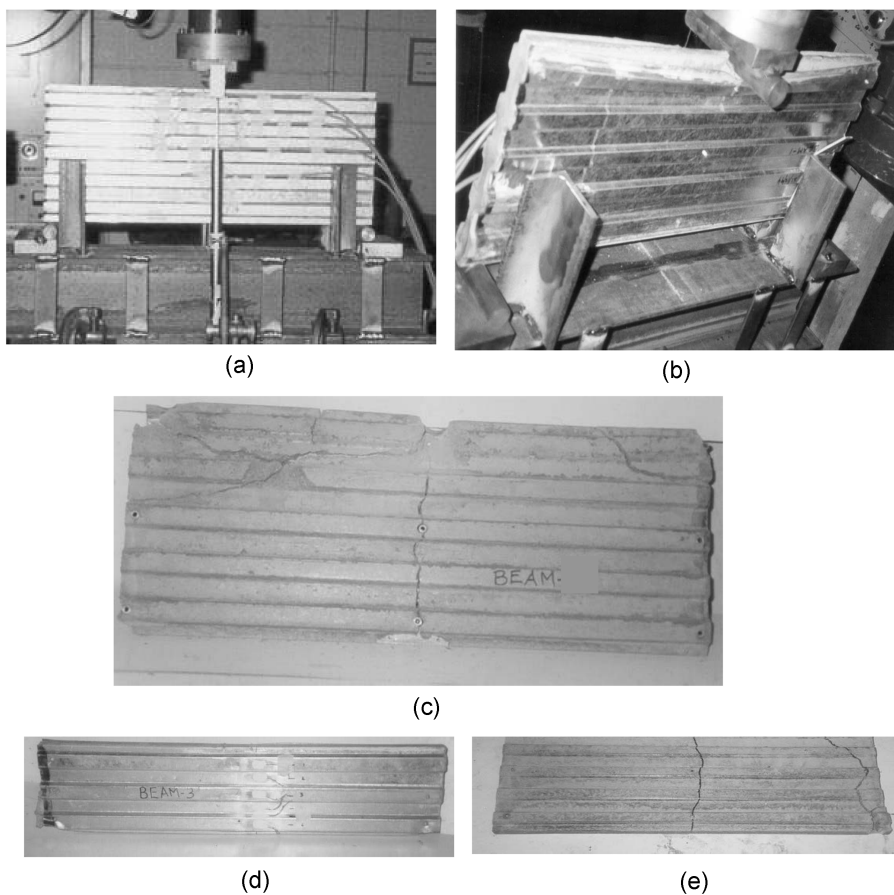
Fig. 7 (a) Model A1 before failure, (b) Model A1 after failure, (c) Crack pattern in Model A1, (d) Failure of model B3, (e) Crack pattern in Model B3
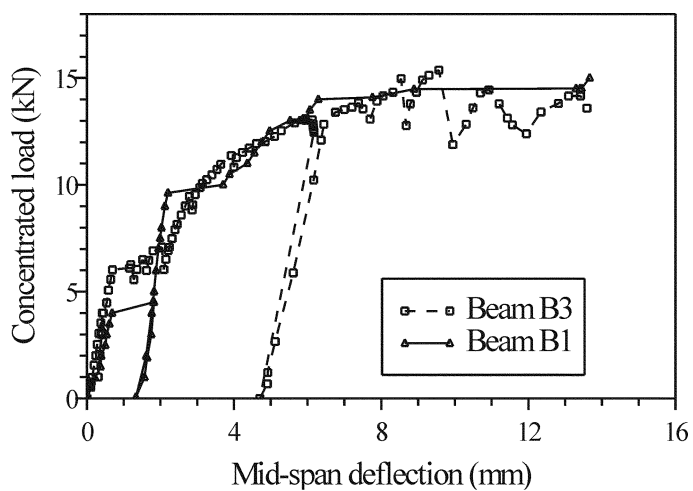

Fig. 8 Central load-deflection responses (B1 and B3)
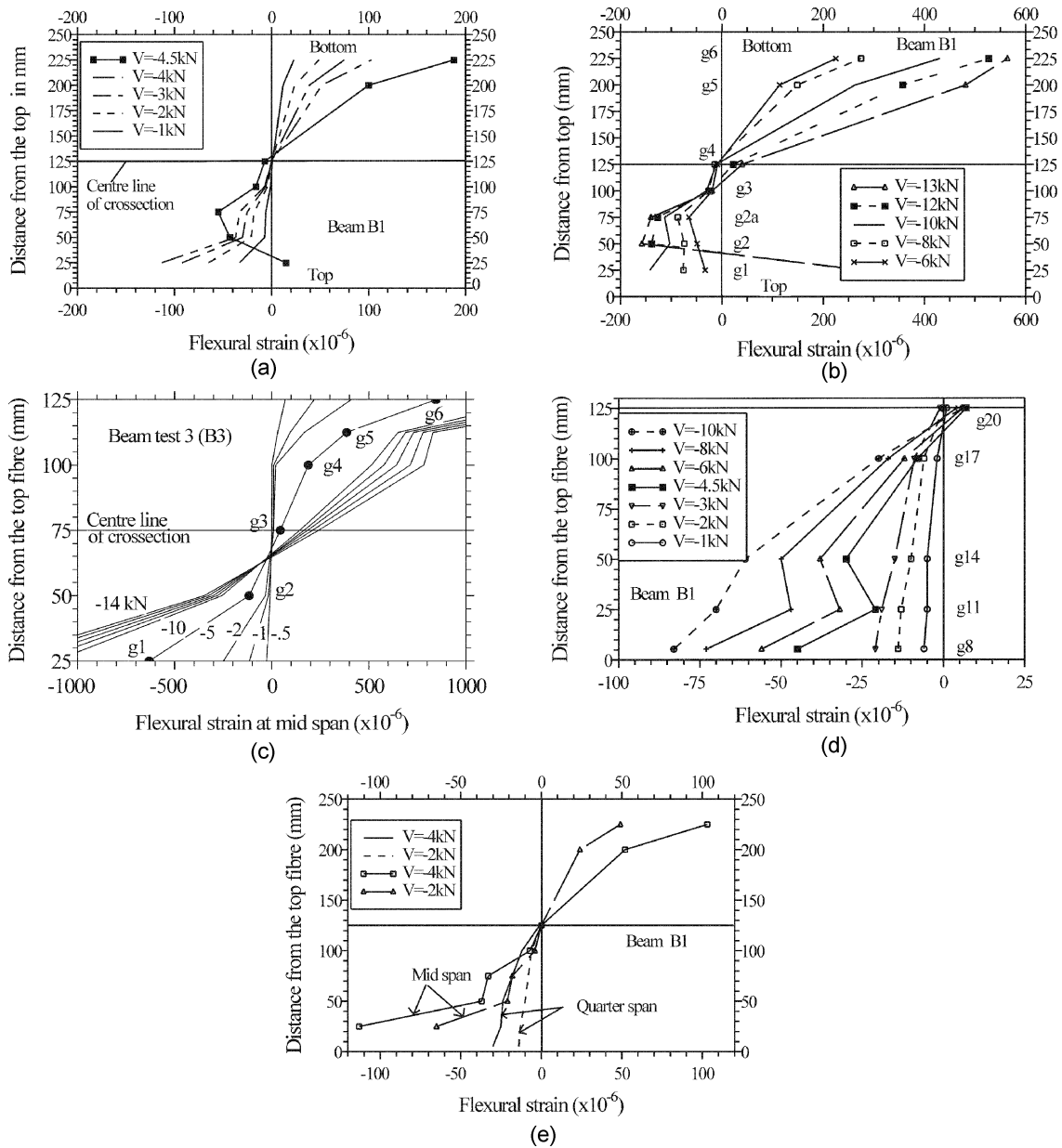
Fig. 9 (a) Variation of flexural strains at mid span in B1 (V: applied load), (b) Variation of flexural strains at mid span in B1 (V: applied load), (c) Variation of flexural strains at mid span (B3), (d) Flexural strain at quarter-span (B1), (e) Mid and quarter span comparison (B1)

around 14 kN.

After concrete cracking, the position of zero strains for both DSCE model beams started to change its position gradually and moved towards the compression zone (Figs. 9). This was an indication of the shifting of the neutral axis in the post-cracking stages up to failure.

2.5.2. Flexural strains at quarter span

The variation of flexural strains across the depth of the beam was similar to that at mid span (Fig. 9d). The flexural strain at the crest position (gauge g-11) was lower than that at the trough position (gauge g-14) although g-11 was furthest from the neutral axis. Therefore, the strain variation was affected by the profiled shape of the cross-section. However, at lower levels this was not apparent. This was perhaps due to the broken sheet-concrete interface bond. The flexural strains at mid and quarter span are compared for DSCE model B1 in Fig. 9(e). The strains at quarter span were lower than those at mid span as expected.

2.5.3. Principal strains

The variation of principal strains calculated from rosette (R) gauges in DSCE model B1 (Series B) is shown in Fig. 10(a). Analysis of strains at trough and crest positions revealed that the strains were higher near the neutral axis compared to those near the top fibre as expected. The principal directions were found to increase from the outer fibres (around 4°) towards the neutral axis (around 42°) (Fig. 10b).

2.5.4. Shear strains

The variation of shear strain calculated from rosette (R) gauges in DSCE model B1 (Series B) confirmed zero shearing strain at the outer fibres of the beam section with maximum at the neutral axis (Fig. 11). The variation was not parabolic due to the profiled shape of the cross section. The trough positions showed higher strains than the crest positions.

The analysis of strains showed that the strain characteristics in DSCEs were affected by the cracking of concrete, sheet-concrete debonding, partial composite action especially in the post-cracking stage and profiled nature of the cross-section.

3. Analytical investigations

The strength of a beam may be governed by flexure, shear, diagonal splitting caused by shear or by bearing at the supports. The mode of failure is a function of the dimensions of the beam, such as span/depth, shear span/depth, depth/width (slenderness) ratios and also on the reinforcement in the beam. According to CIRIA Guide 2 (1977), if the span/depth ratio of a simply supported beam is less than 2
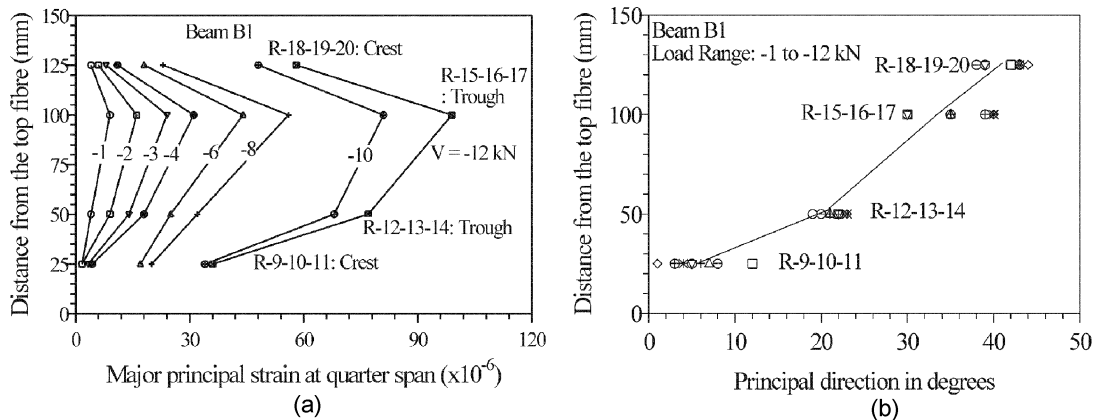

Fig. 10 (a) Variation of principal strain (B1), (b) Variation of principal direction (B1)
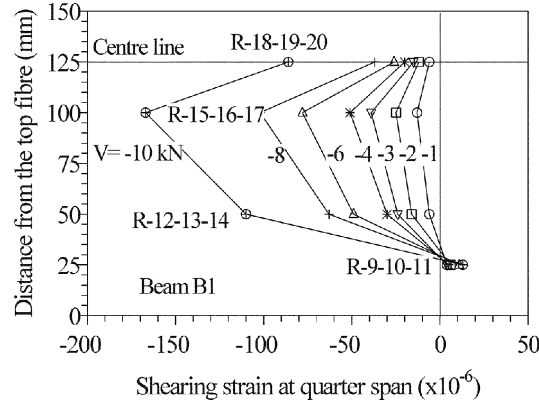
Fig. 11 Variation of shearing strain (B1)

the beam should be considered as a deep beam. According to this recommendation, DSCE models did not fall into the deep beam category but models with span/depth ratios (*b/a*) of 2.36 and 2.46 might show deep beam characteristics (Table 1).

The DSCE models were simplified according to Oehlers *et al.* (1994) as an equivalent rectangular beam as shown in Fig. 12. The effective width of the concrete in DSCE models, t_{eqc}, was taken as the width of the equivalent rectangular block that enclosed the same area as the profiled cross-section. The equivalent thickness of steel skins (t_{eqs}) was calculated as:

$$t_{eqs} = \alpha t_s \tag{1}$$

where t_s was the thickness of the steel and α was the ratio of developed length of a corrugation of the profiled steel sheet to its projected length. The values of α and t_s were 1.198 and 0.45 mm, respectively for the profiled sheeting used in this study.

3.1. Analytical model for shear strength

3.1.1. Existing equations

The truss analogy was developed around the turn of the Century (Wood 1990), as a means of relating the applied shear to the tensile stresses in the web reinforcement of reinforced concrete beams. The
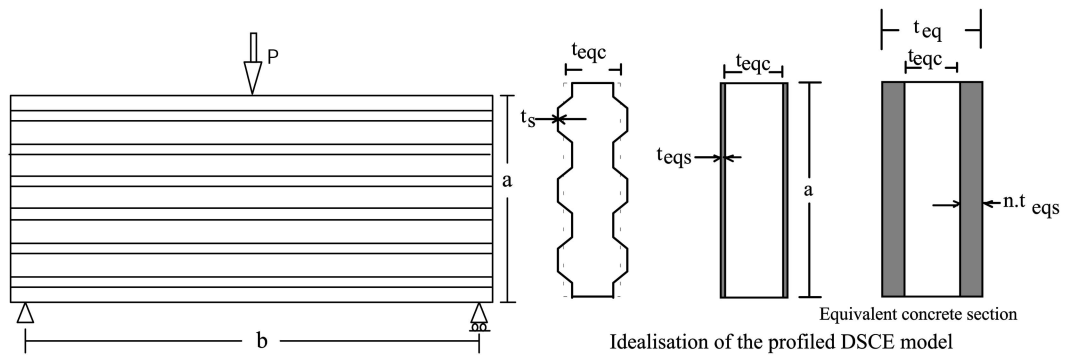

Fig. 12 Equivalent rectangular beam

beam was idealised as a truss, where the bottom chord represented the longitudinal reinforcement, the top chord represented concrete in the compression zone, compression web members by concrete in the web and the tension web members by the stirrups. The relationship between the average shear stress in the beam, v, and the tensile stress in the vertical web reinforcement f_v, assuming the angle between the longitudinal axis and the compression strut to be 45°, was written as:

$$v = r f_v \tag{2}$$

where r was the web reinforcement ratio. Eq. (2) was later modified to take account of the contribution of the uncracked concrete in the compression zone and deviation of the direction of diagonal compression from 45° in the actual situation as:

$$v = C + r f_v \tag{3}$$

where C was the concrete contribution dependent on the quality of concrete and amount of web reinforcement.

The simplest expression similar to Eq. (3) given in ACI 318-83 (1983) for calculating the nominal unit shear strength of beams subjected to flexure and shear is:

$$v_n = 0.167 \sqrt{f_c'} + \rho_n f_{yw} \qquad \text{in MPa} \tag{4}$$

where v_n is the nominal unit shear strength, ρ_n is the reinforcement ratio for the vertical web reinforcement and f_{yw} is the yield stress of the vertical web reinforcement.

The nominal shear strength (v_{nw}) of walls presented in Appendix A of ACI 318-813 is closely related to the nominal shear strength of beams as defined in Eq. (5).

$$v_{nw} = \alpha_c \sqrt{f_c'} + \rho_n f_{yw} \tag{5}$$

where α_c varies linearly from 0.25 for walls with an aspect ratio h_w / a_w (h_w = height of the wall and a_w = width of the wall) less than 1.5, to 0.167 for walls with an aspect ratio greater than 2.0. If α_c is set at the lower bound of 0.167, Eq. (5) becomes identical to Eq. (4). The upper bound of the nominal shear strength of walls (v) should be:

$$v = 0.67 \sqrt{f_c'} \tag{6}$$

3.1.2. Full composite shear strength model for DSCE

Eq. (5) can be used to determine the shear resistance of the DSCEs by using the values of shear stress (v) suggested by ACI 318-83. The main problem associated with the DSCEs is the degree of compositeness between sheeting and concrete core and the role of sheeting as web reinforcement resisting diagonal tension. Assuming full composite action and considering the cross-section of the DSCE as an equivalent concrete beam (Fig. 12), the shear resistance V_{wb} of the DSCEs is given by:

$$V_{wb} = va[t_{eqc} + 2n t_{eqs}] = \varphi \sqrt{f_c'} \cdot a[t_{eqc} + 2n t_{eqs}] = \varphi \sqrt{f_c'} \cdot a[t_{eqc} + 2n \alpha t_{eqs}] \tag{7}$$

where n is the modular ratio. The values of φ can be taken as recommended by ACI 318-83

depending on *b/a* of DSCE. Eq. (7) did not take into consideration the effect of steel skins as shear reinforcement and a factor β was incorporated to the full composite shear resistance Eq. (7). The modified shear resistance equation for DSCEs was presented as:

$$V_{wb} = \beta\varphi\sqrt{f_c'} \cdot a[t_{eqc} + 2n\,\alpha t_{eqs}] \qquad (8)$$

The value of β was determined from the shear resistance of the tested DSCE models.

3.1.3. Comparison between analytical and model tests

Analytical and experimental shear strengths and modes of failure, either shear or flexure, are compared in Table 2. Comparatively deeper DSCE models A1 (*b/a* of 2.36), B1, B1a and C1 (*b/a* of 2.46) were dominated by shear behaviour and test shear resistances were close to the full composite shear resistance based on Eq. (7). The ratio of analytical (Eq. 7) to experimental shear resistance ranged between 0.78 and 0.84. Higher experimental shear resistance was attributed to the neglect of the contribution of the steel skins as shear reinforcement in Eq. (7). The shear resistance contribution factor, β, to be used in Eq. (8) for the DSCE models tested in this study ranged between 1.19 and 1.28 (Table 2).

All other comparatively slender DSCE models with *b/a* ranging between 2.95 and 5.90 showed flexure mode of failure and consequently registered higher shear loads than those predicted from Eq. (7). The ratio of analytical (Eq. 7) to test shear at flexural failure ranged between 0.35 and 0.60. This indicates that Eq. (7) (derived for shear resistance) can not be used to predict the ultimte load of DSCE beams failed in flexure.

Table 2 Comparison of analytical and test shear strength

	Test	Shear resistance kN		Ratio	β*
	Failure load (kN)	Eq. (7) ($\varphi = 0.167$) (i)	Test (ii)	Analytical/Expt. (i)/(ii)	Eq. (8)
		Series A			
A1	14.8 (S)	6.2	7.4	0.84	1.19
A2	14.0 (F)	3.5	7.0	0.50	
		Series B			
B1	15.4 (S)	6.4	7.7	0.83	1.20
B1a	15.2 (S)	6.4	7.6	0.84	1.19
B2	29.3 (F)	5.3	14.6	0.38	
B2a	28.1 (F)	5.3	14.0	0.38	
B3	15.0 (F)	3.7	7.5	0.49	
B3a	14.6 (F)	3.7	7.3	0.51	
B4	9.1 (F)	2.7	4.5	0.60	
B4a	8.9 (F)	2.7	4.5	0.60	
		Series C			
C1	16.4 (S)	6.4	8.2	0.78	1.28
C2	21.0 (F)	3.7	10.5	0.35	
C3	11.6 (F)	2.7	5.8	0.41	

S: shear mode of failure *F*: flexure mode of failure *only for shear mode

3.2. Analytical model for the flexural strength

Analytical models for the flexural strength of DSCEs considering full and partial composite action were developed based on the model proposed by Oehlers *et al.* (1994) and Hossain (2003). A DSCE beam as shown in Fig. 12 subjected to load *P* was considered**.** The design point was taken as the position of maximum moment at a distance *b*/2 and *b*/3 from the end of the DSCE beam for single and two point loading respectively. Up to the limit of generated interface bond force not exceeding the interface bond strength, the DSCE beam would exhibit full interaction and there would be no slip across the steel-concrete interface. The same strain distribution would exist in sheeting and concrete with neutral axis of both steel and concrete sections, N, coincident to each other as shown in Figs. 13(a-b). If the maximum moment capacity was reached without the interface bond force exceeding the interface bond strength then the beam exhibited full composite action or full interaction.

But in reality, it was difficult to have full interaction in DSCE beams. DSCE beams exhibited partial interaction with slip occurring across the interface due to the interface bond force exceeding the interface bond strength. As a result, there would be a step change, ε_{sl} between the strain in sheeting and concrete as shown in Fig. 13(c). The position of the neutral axis for concrete N_c would be different from that for the steel sheeting N_s. According to Oehlers (1992), the slip strain was assumed to be constant throughout the depth of the beam which lead to a uniform slip at the ends.

The flexural strength of the DSCE beams was determined by considering the distribution of forces in concrete and steel sections. The distribution of forces in individual concrete and steel sections is shown in Fig. 14.

3.2.1. Partial shear connection (PSC)

For partial shear connection, $N_c \neq N_s$. Considering the equilibrium of forces in the concrete $P_c = P_b$, the expression for N_c was written as:

$$N_c = \frac{P_b}{0.85f_c' t_{eqc}} \tag{9}$$

where P_c = compressive force due to concrete. The interface bond force (P_b) at the location of maximum moment for the DSCE beam derived from interface bond stress (f_b) could be written as: $P_b = \Sigma_o \times f_b$, where Σ_o = cross-sectional perimeter of steel sheeting in contact with concrete and $x = b/2$ or $b/3$.
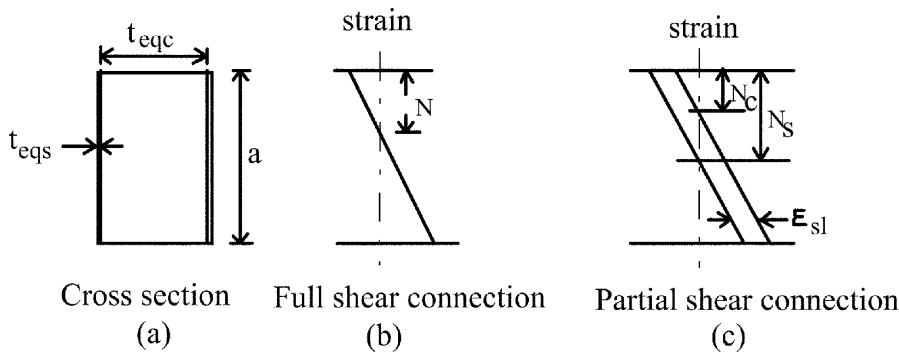

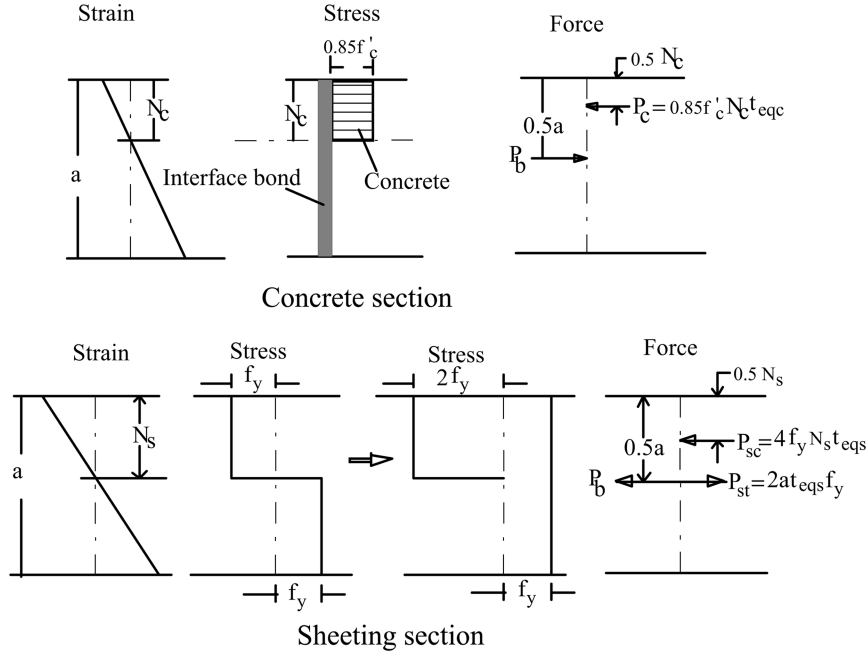Fig. 13 Strain distribution in full and partial shear connection in DSCE

Fig. 14 Distribution of forces in flexural action of DSCE

The maximum shear bond stress (Patrick 1990) at the sheet-concrete interface due to mechanical interlock in the form of different types of embossment rolled into the sheet ranges from 0.2 to 0.5 N/mm^2. For plain profile sheeting with no embossments, a value of 0.1 N/mm^2 can be used.

From the equilibrium of steel section, $P_{sc} + P_b = P_{st}$; the depth of the neutral axis N_s was derived as:

$$N_s = \frac{2t_{eqs}af_y - P_b}{4f_yt_{eqs}} \tag{10}$$

where P_{sc} = force due to compressive steel, and P_{st} = force due to tensile steel.

The moment capacity (M_{pc}) of the DSCE beams with partial interaction should be determined based on Eq. (11).

$$M_{pc} = f_yt_{eqs}a^2 - 2f_yt_{eqs}N_s^2 - 0.425f_c't_{eqc}N_c^2 \tag{11}$$

3.2.2. Full shear connection (FSC)

For full shear connection, $N_c = N_s$, thus equating Eq. (9) and Eq. (10), the bond strength $(P_b)_{fc}$ required to achieve full shear connection, was derived as:

$$(P_b)_{fc} = \frac{1.70t_{eqs}af_yf_c't_{eqc}}{0.85f_c't_{eqc} + 4f_yt_{eqc}} \tag{12}$$

Substituting the value of P_b from Eq. (12) in Eqs. (9) and (10) would allow the determination of N_c and N_s. The moment capacity for full shear connection could be obtained by substituting the value of N_c and N_s in Eq. (11).

Table 3 Analytical and test comparison

Test no.	Analytical (Eq. (11) & (12)) FSC			Analytical (Eq. (11)) PSC			Test Load P	Ratio Analytical/Test loads	
	Moment kN-mm	Load kN	f_b required	Moment kN-mm	Load kN	f_b assumed	kN	FSC	PSC
Series A									
A1	8174	55.0	0.168	7870	53.0	0.1	14.8 (S)	3.72	3.58
A2	2563	17.4	0.168	2468	16.7	0.1	14.0 (F)	1.24	1.19
Series B									
B1	7725	52.4	0.187	7314	49.6	0.1	15.4 (S)	3.40	3.22
B1a	7725	52.4	0.187	7314	49.6	0.1	15.2 (S)	3.45	3.26
B2	5365	36.4	0.187	5079	34.4	0.1	29.3 (F)	1.24	1.17
B2a	5365	36.4	0.187	5079	34.4	0.1	28.1 (F)	1.29	1.22
B3	2629	17.8	0.187	2489	16.9	0.1	15.0 (F)	1.18	1.15
B3a	2629	17.8	0.187	2489	16.9	0.1	14.6 (F)	1.21	1.15
B4	1341	9.1	0.187	1270	8.6	0.1	9.1 (F)	1.00	0.95
B4a	1341	9.1	0.187	1270	8.6	0.1	8.9 (F)	1.02	0.97
Series C									
C1	7725	78.6	0.280	6937	70.6	0.1	16.4 (S)	4.79	4.30
C2	2629	26.7	0.280	2361	24.0	0.1	21.0 (F)	1.27	1.14
C3	1341	13.6	0.280	1204	12.2	0.1	11.6 (F)	1.17	1.05

3.2.3. Comparative study of analytical and test results

The ultimate moment capacity and the resulting ultimate load for full and partial sheet-concrete shear connection are compared with those of model tests in Table 3. The interface shear bond (f_b) required to have full shear connection ranged between 0.168 - 0.280 N/mm² for DSCE beams. This value of interface bond can be attained by using sheeting with embossments as shear connectors as confirmed by Patrick (1990). Analytical calculations for partial connection were performed with interface shear bond of 0.1 N/mm², typical for plain sheeting (Patrick 1990). The moment capacity was not found to be sensitive to the interface bond stress.

DSCE models A1, B1, B1a and C1 with b/a of about 2.36 and 2.46 failed at a load which was only one third of the analytically determined flexural capacity as the ratio of analytical to experimental values ranged between 3.40 and 3.79 for FSC while for PSC, they ranged between 3.20 and 4.30. This signified that the beams could not achieve their moment capacity and shear failure dominated as described earlier.

All other beams with b/a ranged between 2.95 and 5.90 showed flexural failure. Good agreement between analytical and test flexural capacity was found (Table 3). The ratio of analytical to test values ranged between 1.0 and 1.29 (for FSC) and 0.95 and 1.222 (for PSC). This signified that these DSCE beams attained their full flexural capacity before failure. Therefore, Eq. (11) with PSC can predict the flexural capacity of DSCEs with reasonable accuracy.

3.3. Full composite linear model for load-deflection response and stiffness for DSCE

To determine the load versus mid span deflection (Series A and B only), the DSCE was considered as elastic and the beam cross-section was transformed into an equivalent concrete section (Fig. 12). The

moment of inertia I_{com} of the equivalent concrete section was derived as:

$$I_{com} = \frac{a^3}{12}[t_{eqc} + 2nt_{eqs}] = \frac{a^3}{12}[t_{eqc} + 2n\alpha t_s] = \frac{a^3 \cdot t_{eq}}{12} \tag{13}$$

where t_{eq} = total width of the equivalent concrete DSCE beam. The total deflection (Δ) under the load of a simply supported beam subjected to a concentrated load (P) at the centre was derived as per Timoshenko *et al.* (1982) with some modification for DSCE as:

$$\Delta = \frac{Pb^3}{48E_c \cdot I_{com}} + \frac{P}{E_c t_{eq}}\left[\frac{b}{2a}\left(\frac{3(1+v_c)}{2} - \frac{3}{10} - \frac{3v_c}{4}\right) - 0.21\right] \tag{14}$$

Using the value of I_{com} from Eq. (13), Eq. (14) was written as:

$$\Delta = \frac{P}{4E_c \cdot t_{eq}}\left[\frac{b}{a}\right]^3 + \frac{P}{4E_c \cdot t_{eq}}\left[(2.4 + 1.5v_c)\left(\frac{b}{a}\right) - 0.84\right] \tag{15}$$

The first term in Eq. (15) represented deflection due to bending and the second term represented deflection due to shear. However, Eq. (15) did not take into account the effect of local deformation at the support and was valid only within the linear stages of P-Δ response.

4. Comparative study of different analyses

The ultimate load and pre-cracking stifness (P-Δ response) of DSCEs from test and analytical prediction are summarised in Table 4. Analytical stiffnesses of DSCEs (Series B) were found to be in

Table 4 Ultimate load and pre-cracking stiffness of DSCEs

Test no.	Test		Analytical (Anal.)		Ratio	
	Load kN	Stiffness kN/mm	Load kN PSC (Eq. (11))	Stiffness kN/mm (Eq. (15))	Stiffness Test/Anal.	Load Test/Anal.
A1	14.8 (S)	72	14.7*	127	0.57	1.00
A2	14.0 (F)	15	16.7	28	0.54	0.84
B1	15.4 (S)	93	15.2*	115	0.81	1.01
B1a	15.2 (S)	91	15.2*	115	0.79	1.00
B2	29.3 (F)	60	34.4	72	0.83	0.85
B2a	28.1 (F)	56	34.4	72	0.78	0.82
B3	15.0 (F)	22	16.9	28	0.79	0.89
B3a	14.6 (F)	21	16.9	28	0.75	0.86
B4	9.1 (F)	8	8.6	11	0.73	1.06
B4a	8.9 (F)	9	8.6	11	0.82	1.03
C1	16.4 (S)	-	15.2*	-	-	1.08
C2	21.0 (F)	-	24.0	-	-	0.88
C3	11.6 (F)	-	12.2	-	-	0.95

*Based on shear failure (Eq. (8) with $\beta = 1.19$)

reasonable agreement with the test results although test stiffnesses were lower. The higher stiffness in analytical model was expected as it was based on full composite action between steel and concrete. The ratio of test to analytical ranged between 0.73 and 0.83. Analytical Eq. (15) was good in predicting the pre-cracking stiffness of DSCEs despite their overprediction. On the other hand poor agreement in Series A (ratio ranged between 0.54 and 0.57) was attributed to the bearing failure at the point of application of concentrated load which significantly affected the load-deflection response.

Analytically predicted ultimate loads either based on shear (Eq. (8)) or flexural (Eq. (11) with PSC) mode of failure were found to be in good agreement with the test results as the ratio of test to analytical load ranged between 0.84 and 1.08 (Table 4).

5. Conclusions

Thirteen small-scale model tests revealed the behaviour of double skin composite elements (DSCE) undergoing bending and shear deformations. The failure mode of DSCEs, either by shear or flexure, was found to be dependent on the span to depth ratio (b/a) that ranged between 2.36 and 5.90. For comparatively shallow DSCEs, the failure was dominated by flexure whereas shear dominated failure was observed for comparatively deep DSCEs. Model tests suggested that adequate boundary connections should be provided to fully mobilise the flexural and shear strength of DSCEs and to avoid localised bearing failure at the supports or at the loaded points.

The strain conditions within DSCEs were excellently demonstrated by tests. The general strain distributions were found to be similar to those of ordinary beams. The flexural strains were maximum at the outer fibres and zero at the neutral axis. The position of the neutral axis gradually shifted towards the compression zone as the cracking continued. The shearing strain was found to be maximum at the neutral axis and zero at the outer fibres as expected. The effect of profile geometry was observed on flexural, shear and principal strains. The trough sections were more highly stressed than the crest sections. The direction of the principal stresses was changed from the outer layers (1 to 10 degree to the horizontal) to the neutral axis (40 to 44 degree to the horizontal). This actually reflected the interaction of flexural and shearing stresses across the depth of the DSCE beams.

Analytical models for shear and flexural strengths for DSCEs were developed. Comparative study of the analytical and model tests suggested that the flexural capacity of the DSCEs could be determined by using the proposed analytical equations. The analytical model developed for linear load-deflection response was found good for determining the initial or pre-cracking stiffness of the DSCEs.

References

ACI 318-813 (1983), Building Code Requirements for Reinforced Concrete ACI Committee 318, ACI, Detroit, 111 pp.

Adams, P.F. (1987), "Steel-concrete composite structural system", *POAC, 87, 9th International Conference on Port and Ocean Engineering under Arctic Conditions*, Fairbanks, Alaska, 1-2.

Bradford M.A., Wright H.D. and Uy B. (1998), "Short and long-term behaviour of axially loaded composite profiled walls", *Proc. Institution of Civil Engineers, Structures and Buildings*, **128**, Feb. 26-37.

CIRIA Guide 2 (1977), "The design of deep beams in reinforced concrete", Ove Arup, London, January.

Gallocher, S.C. (1993), "The behaviour of composite wall with profiled steel sheeting", PhD Thesis, University of Strathclyde, Glasgow, UK.

Hossain K.M.A. (2000), "Axial behaviour of pierced profiled composite walls", *IPENZ Transaction*, **27**(1)/Civ, 1-7, New Zealand.

Hossain K.M.A. (2003), "Experimental and theoretical behaviour of thin walled composite beams", *Electronic J. Struct. Eng., An Int. J.*, **3**, 117-139, EJSE International.

Hossain K.M.A. and Wright H.D. (1998a), "Shear interaction between sheeting and concrete in profiled composite construction", *Proce. of the Australasian Structural Engineering Conference*, Auckland, 30 Sept.-2 October, vol. 1, pp. 181-188 (ISBN 0-473-05481-7).

Hossain K.M.A. and Wright H.D. (1998b), "Performance of profiled concrete shear panels", *J. Struct. Eng.*, ASCE, **124**(4), April, 368-381.

Hossain, K.M.A. and Wright, H.D. (1995), "Composite walling with special reference to the stabilisation of building frames", *Proc. Nordic Steel Construction Conference*, 531-538, Malmo, Sweden, June 19-21.

Hossain, K.M.A. and Wright, H.D. (2004a), "Experimental and theoretical behaviour of double skin composite walls under in-plane shear", *J. Construct. Steel Res.*, **60**, 59-83.

Hossain, K.M.A. and Wright, H.D. (2004b), "Behaviour of composite walls under monotonic and cyclic shear loading", *Struct. Eng. Mech., An Int. J.*, **17**(1), 69-85.

Hossain, K.M.A. and Wright, H.D. (2004c), "Design aspects of double skin composite framed shear walls in construction and service stages", *ACI Struct. J.*, **101**(1), January-February, 94-102.

Link, R.A. and Elwi, A.E.(1995), "Composite concrete-steel plate walls: analysis and behaviour", *J. Struct. Eng.*, ASCE, **121**(2), February, 260-271.

Naraynan, N., Wright, H.D., Evans, H.R. and Francies, R.W. (1987), "Double skin composite construction for submerged tube tunnels", *Steel Construction Today*, **1**, 187-189.

Oehlers, D.J. (1993), "Composite profiled beams", *J. Struct. Eng.*, ASCE, **119**(4), 1085-1100.

Oehlers, D.J., Wright, H.D. and Burnet, M.J. (1994), "Flexural strength of profiled beams", *J. Struct. Eng.*, ASCE, **120**(2), February, 378-393.

Patrick, M. (1990), "A new partial shear connection strength model for composite slabs", *J. Australian Inst. Steel Res.* **24**(3) 2-17.

Timoshenko, S.P. and Goodier, J.N. (1982), *Theory of Elasticity*, McGraw-Hill Book Company.

Wood S.H. (1990), "Shear strength of low-rise reinforced concrete walls", *ACI Struct. J.*, **87**(1), Jan-Feb., 99-107.

Wright, H.D., Oduyemi, T.O.S. and Evans, H.R. (1991), "The double skin composite elements", *J. Construct. Steel Res.*, **19**, 111-132.

Wright H.D. (1998), "The axial load behaviour of composite walling", *J. Construct. Steel Res.*, **45**(3), 353-375.

Wright H.D. and Gallocher S.C. (1995), "The behaviour of composite walling under construction and service loading", *J. Construct. Steel Res.*, **35**(3), 257-273.

Wright, H.D. and Evans H.R. (1995), "Profiled steel concrete sandwich elements for use in wall construction", *Proc. Third International Conference on Sandwich Construction*, Southampton, 12-15 September.

Wright, H.D., Evans, H.R. and Gallocher, S.C. (1992), Composite walling, Composite Construction II, *Engineering Foundation Conference*, Missouri, June 14-19.

Wright, H.D., Hossain, K.M.A., Gallocher, S.C. (1994), "Composite walls as shear elements in tall structures", *Proce. ASCE Structures Congress XII*, Atlanta, GA, USA, April 24-28, pp. 140-145.

Yarushalmi, Y.(1988), "Tests performed on the ASP construction system", The ASP Group, Washington D.C., 32.

Notation

DSCE	: double skin composite element
b, a, w	: effective span, depth and width of DSCE, respectively
f_c', n_c, E_c	: concrete cylinder strength, Poisson's ratio and modulus of elasticity, respectively
f_y, E_s, n_s	: yield strength, modulus of elasticity and Poisson's ratio of steel sheet, respectively
t_s	: thickness of profiled steel sheet
t_{eqs}	: thickness of profiled steel skins as an equivalent plain rectangular sheet
α	: ratio of developed length of a corrugation of profiled sheet to its projected length

n	: modular ratio
P_b, f_b	: interface bond force and bond stress respectively
t_{eqc}	: effective width of profiled concrete as equivalent rectangular section
P or V	: applied concentrated load on DCSE
Δ	: total deflection of DSCE beam at the point of concentrated load (P)
PSC, FSC	: partial shear connection and full shear connection respectively
M_{pc}	: moment capacity of DSCE beams with partial interaction (shear connection)
I_{com}	: moment of inertia of the equivalent concrete section
t_{eq}	: total width of the equivalent concrete section of DSCE beam
CC	